Temperature dependence of band gaps in semiconductors: Electron-phonon interaction

J. Bhosale and A. K. Ramdas
Physics Department, Purdue University, 525 Northwestern Avenue, West Lafayette, Indiana, USA

A. Burger
Fisk University, Department of Life and Physical Sciences, Nashville, Tennessee, USA

A. Muñoz
MALTA Consolider Team, Departamento de Física Fundamental II, and Instituto de Materiales y Nanotecnología, Universidad de La Laguna, La Laguna, Tenerife, Spain

A. H. Romero
CINVESTAV, Departamento de Materiales, Unidad Querétaro, Querétaro, Mexico and Max-Planck-Institut für Mikrostrukturphysik, Weinberg 2, Halle, Germany

M. Cardona, R. Lauck, and R. K. Kremer*
Max-Planck-Institut für Festkörperforschung, Heisenbergstrasse 1, Stuttgart, Germany
(Received 4 October 2012; published 26 November 2012)

We have theoretically investigated, by *ab initio* techniques, the phonon properties of several semiconductors with chalcopyrite structure. Comparison with experiments has led us to distinguish between materials with d electrons in the valence band (e.g., $CuGaS_2$, $AgGaS_2$) and those without d electrons (e.g., $ZnSnAs_2$). The former exhibit a rather peculiar nonmonotonic temperature dependence of the energy gap which, so far, has resisted cogent theoretical description. We analyze this nonmonotonic temperature dependence by fitting two Bose-Einstein oscillators with weights of opposite sign leading to an increase at low temperatures and a decrease at higher temperatures and find that the energy of the former correlates well with characteristic peaks in the phonon density of states associated with low-energy vibrations of the d-electron elements. We hope that this work will encourage theoretical investigations of the electron-phonon interaction in this direction, especially of the current *ab initio* type.

DOI: 10.1103/PhysRevB.86.195208 PACS number(s): 63.20.D−, 63.20.dk, 68.35.bg

I. INTRODUCTION

In the past decade *ab initio* calculations of the electronic properties and especially the band gaps of semiconductors have experienced considerable development. Generally, these calculations are performed for $T = 0$. Comparison of these calculations with experimental data, however, requires consideration of the zero-temperature vibrational amplitudes as well as the effects of finite temperature. Inclusion of these effects is computationally rather cumbersome and therefore it is often erroneously assumed that zero temperature is equivalent to zero-point vibrational amplitude.[1] In recent years, a number of calculations of the effects of lattice vibrations on the gaps and other electronic properties have been performed using either semiempirical[2,3] or *ab initio* methods.[4] This work has led to the realization that the lowest gaps usually decrease with increasing temperature,[2,3] although the opposite effect is also observed in a few exceptional cases.[1,5] The effects under consideration, due to electron-phonon interaction, can usually be represented by lattice vibrations which correspond to one or more Bose-Einstein oscillators.[1,5,6]

Manoogian and Leclerc suggested an empirical equation to describe the energy gap temperature variation. It included terms to account for the effects of lattice dilation and electron-phonon interaction.[7] This so-called Manoogian-Leclerc equation comprises an Einstein oscillator as a first approximation to describe the effect of the lattice vibrations. Manoogian and Wooley subsequently demonstrated that the Varshni empirical model[8] is a second-order approximation of the Bose-Einstein term in the Manoogian-Leclerc equation.[9] More recently Pässler proposed an analytical description of the energy gap temperature dependence wherein within the regime of dominant electron-phonon interaction the electron-phonon spectral function is described by analytical functions up to a certain cutoff.[10] This assumption allows us to derive analytical expressions for the temperature variation of the gap which can be tested against experimental data. It has recently been shown using a Debye model that at very low temperatures the gap vanishes like T^4.[11] For a detailed compilation and a discussion of the various approaches to model the temperature dependence of the gaps, see, e.g., the discussion in Ref. 12.

Most of the experimental results for the temperature dependence of gaps have been obtained for binary semiconductors.[1] In recent years, however, ternary materials such as those with chalcopyrite structure have begun to be investigated. Among the chalcopyrites under investigation are II-IV-V_2 compounds (e.g., $ZnGeAs_2$) and those in which the divalent cation is replaced by either monovalent copper or silver (e.g., $MGaX_2$, M = Cu, Ag; X = S, Se, Te). Whereas the temperature dependence of the gaps of the II-IV-V_2 compounds exhibits the standard behavior which can be modeled by a single Bose-Einstein oscillator, the electronic gaps of the Cu and

Ag chalcopyrites often show anomalous temperature behavior with a maximum at low temperatures followed by a decrease of the gap energy above that maximum or sometimes an extended flat plateau at low temperatures (see Figs. 2–4 below). In the literature the drop of the electronic gap below the maximum has often been ascribed to the combined effect of thermal expansion and the volume dependence of the gap (see, e.g., Ref. 13 and references therein). However, a convincing scheme to understand the occurrence of the low-temperature gap decrease has not been suggested, nor has a quantitative picture for the magnitude of the gap decrease been developed on the basis of the volume dilation mechanism. On the other hand, temperature-dependent effects due to the presence of the d-like valence electrons ($3d$ for Cu and $4d$ for Ag) and their admixture with the usual p-like counterparts (e.g., $4p$ for Se, $5p$ for Te) are generally ignored. The observation that the nonmonotonic temperature dependence is particularly noticeable in the chalcopyrites involving Ag $4d$ valence electrons led us to suggest that this effect is related to p-d-electron hybridization. In this paper we will reanalyze published gap versus temperature data of a series of related chalcopyrites with d electrons present or absent. Additionally, we re-measured the temperature dependence of the gap of several Ag and Cu chalcopyrites with a new experimental wavelength-modulated reflectivity setup and analyzed it with a model assuming two Bose-Einstein oscillators. For the Ag chalcopyrites we find a clear correlation of their frequencies with results of new *ab initio* calculations of the phonon dispersion relations and the phonon density of states (PDOS). Below we will argue that for Cu chalcopyrites the nonmonotonic behavior is also present, but significantly weaker than in the Ag compounds. We ascribe this difference to the different degree of p-d hybridization which is modulated by the electron-phonon interaction and subject to details of the phonon spectrum.

In order to surmise the degree of valence electron hybridization we have plotted in Fig. 1 the relevant valence electron energies of the various elements involved.[14] While in the $MGaX_2$ (M = Cu, Ag; X = S, Se, Te) there is a close proximity of the d levels of Cu and Ag to the p levels of the chalcogen atoms enabling enhanced p-d hybridization, the d levels of Zn and Cd are lifted in energy, being considerably separated from the occupied p levels.

The electron-phonon interaction depends critically on the amplitude of the phonons and the corresponding coupling constants. Unfortunately, because of computational complications due to the size of the unit cell and k-point convergence issues, calculations of the corresponding electron-phonon interaction coefficients are difficult and rare. The phonon amplitudes, however, are accessible with great precision from *ab initio* calculations of the electronic structure. Recently we have studied the lattice and thermal properties of $CuGaS_2$ in more detail by means of *ab initio* calculations.[15] Applying analogous computational techniques we have extended these calculations and obtained the phonon dispersion relations of $AgGaX_2$ (X = S, Se, Te) as well as of MYX_2 (M = Zn, Cd; Y = Ge, Sn; X = P, As, Sb). Using these results we have analyzed literature data and new highly resolved gap versus temperature data by fitting a model proposed by Göbel *et al.* for CuX (X = Cl, Br) and subsequently applied to CuI by Serrano *et al.*[5,6] Without any further assumption about thermal expansion

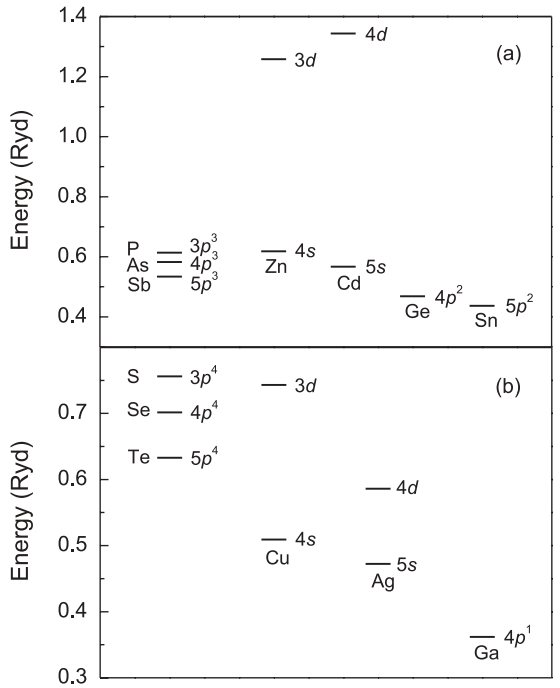

FIG. 1. Relevant valence electron energies of the various elements in the chalcopyrite compounds according to Ref. 14. (a) MYX_2 (M = Zn, Cd; Y = Ge, Sn; X = P, As, Sb). (b) $MGaX_2$ (M = Cu, Ag; X = S, Se, Te). Note the proximity of the $3d$ and $4d$ energy levels of Cu and Ag to the valence p levels of the chalcogenides.

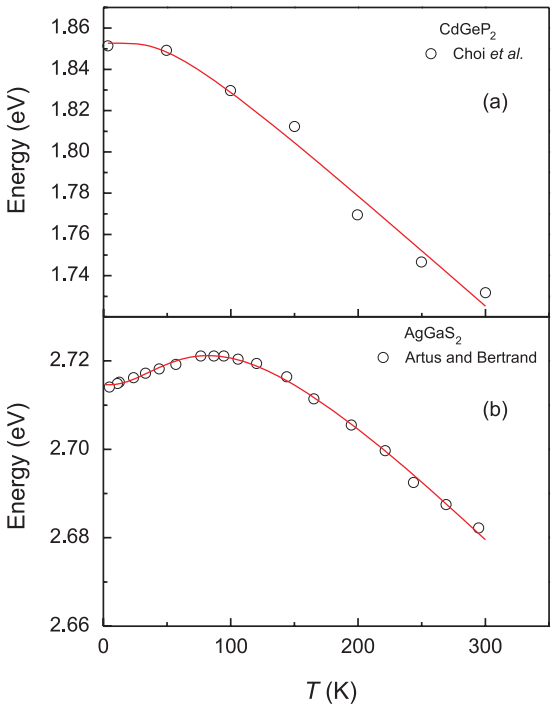

FIG. 2. (Color online) Temperature dependence of the electronic gaps of (a) $CdGeP_2$ (Ref. 16) and (b) $AgGaS_2$ (Ref. 13). The (red) solid lines are fits to the data with a superposition of either one or two Einstein terms (for more details see text).

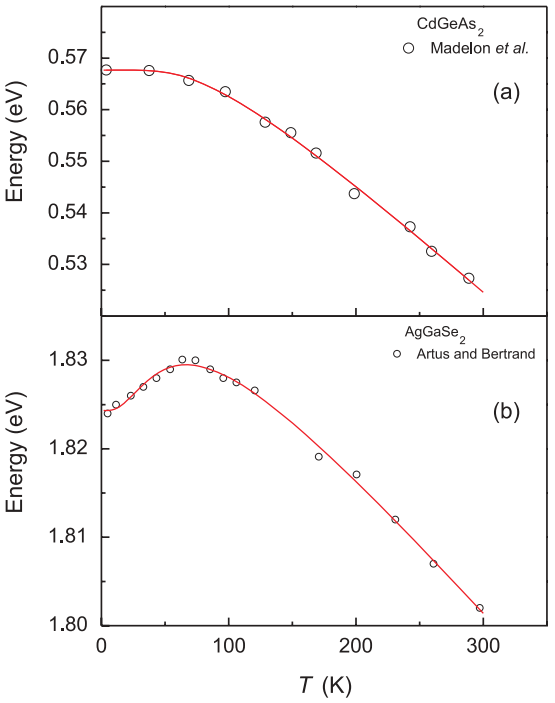

FIG. 3. (Color online) Temperature dependence of the electronic gaps of (a) $CdGeAs_2$ (Ref. 17) and (b) $AgGaSe_2$ (Ref. 13). Similar data for the band gap of $AgGaSe_2$ have recently been reported by Ozaki *et al.* and by Caldéron *et al.*[18,19] The (red) solid lines represent fits to the data with a superposition of either one or two Bose-Einstein terms (for more details see text).

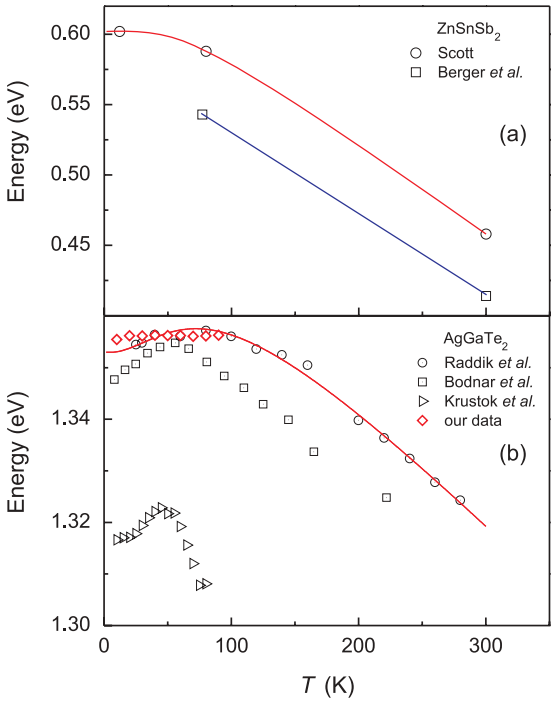

FIG. 4. (Color online) Temperature dependence of the electronic gaps of (a) $ZnSnSb_2$ (Refs. 20,21) and (b) $AgGaTe_2$ (Refs. 22–24). The (red) solid lines are fits to the data of Raadik *et al.* with a superposition of either one or two Einstein oscillators (for more details see text). For $AgGaTe_2$ the energies E_1 and E_2 were not fitted but fixed to the values listed in Table I. The (blue) straight line in (a) is a guide to the eye.

terms, only by including a second low-energy Bose-Einstein oscillator [see Eq. (4) below] this model accounts well for the nonmonotonic temperature dependence of the gaps with the effects of the two oscillators on the gap having different signs, i.e., the low-energy oscillator securing an increase of the gap with increasing temperature. This increase is, however, compensated and finally dominated by the stronger decrease towards higher temperatures.

Figures 2, 3, and 4 display some literature data of the temperature dependence of the electronic gaps of the two classes of chalcopyrites under consideration together with fits assuming one or two Bose-Einstein oscillators. The total temperature variation of the gaps of the Ag chalcopyrites is significantly smaller than that of the Zn and Cd systems. Whereas the former does not exceed ∼2% the latter amounts to up to 30% for $ZnSnSb_2$. All compounds containing Ag exhibit a nonmonotonic temperature dependence with a maximum at around 100 K which is accounted for well by the low-energy Bose-Einstein oscillator with a positive coefficient being smaller in magnitude than the coefficient of the high-energy oscillator, which leads to the standard gap decrease at high temperatures.

The fitted parameters are summarized in Table I. Note that for the $AgGaX_2$ series the fitted frequencies with the negative coefficient decrease when increasing the chalcogen mass (from S via Se to Te), thus reflecting the increasing energy compression of the phonon dispersion relations for the heavier chalcogenides.

II. COMPUTATIONAL AND EXPERIMENTAL DETAILS

The calculations reported here concern the electronic structure, the phonon dispersion relations, and the phonon densities of states (PDOS, including the projections on the three component atoms). The calculations are based on *ab initio* electronic total energy Hamiltonians which use density functional theory and the plane-wave pseudopotential method available within the VASP package.[25] We have used the projector-augmented wave scheme (PAW)[26,27] implemented in this package to take into account the full nodal character of the all-electron charge density in the core region. Basis sets including plane waves up to an energy cutoff of 380 eV were employed in order to achieve highly converged results and an accurate description of the electronic and dynamical

TABLE I. Compilation of the fit parameters obtained from a fit of one/two Bose-Einstein frequencies E_i ($i = 1, 2$), according to Eqs. (1) and (4), to the literature data displayed in Figs. 2–4.

	E_0 (eV)	A_1 (eV)	E_1 (K)	A_2 (eV)	E_2 (K)
$CdGeP_2$	1.89(2)	−0.041(3)	149(74)		
$AgGaS_2$	2.784(6)	−0.074(5)	313(35)	0.004(4)	47(31)
$CdGeAs_2$	0.595(3)	−0.027(4)	246(22)		
$AgGaSe_2$	1.855(3)	−0.035(5)	191(41)	0.004(6)	44(36)
$ZnSnSb_2$	0.66	−0.058	180		
$AgGaTe_2$	1.404(3)	−0.053(3)	280	0.0025(3)	40

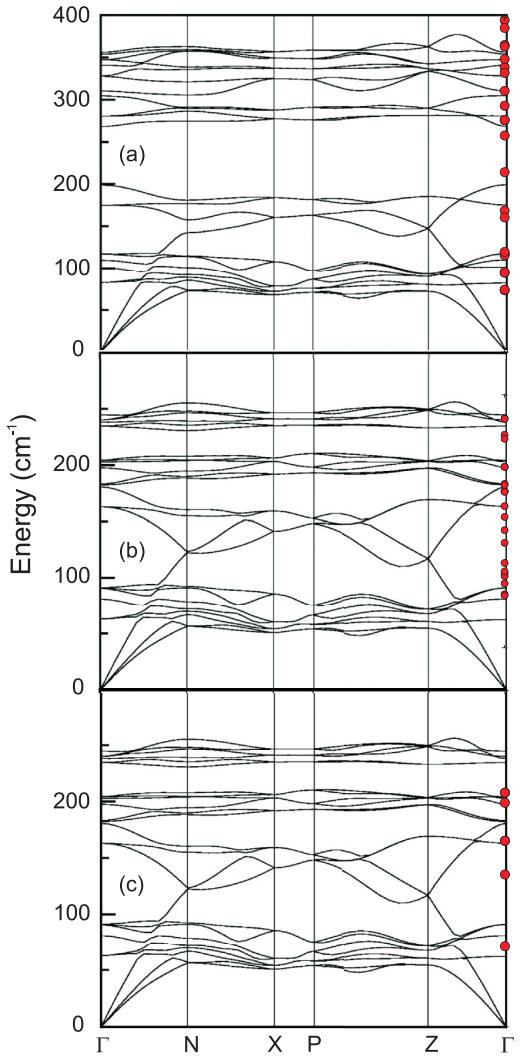

FIG. 5. (Color online) Phonon dispersion relations (PBEsol description) for $CuGaS_2$, $CuGaSe_2$, and $CuGaTe_2$, from top to bottom, respectively. The red circles are Raman and IR frequencies at the Γ point which have been taken from the literature. $CuGaS_2$: Averaged from the data given in Table 4 of Ref. 40; $CuGaSe_2$: averaged from the data given in Table 2 of Ref. 41; Ref. 42.

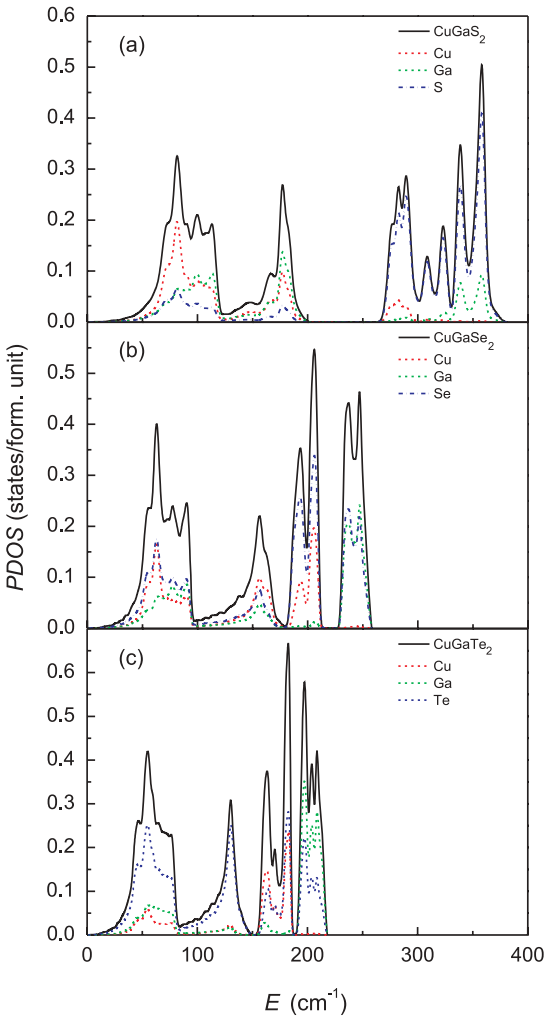

FIG. 6. (Color online) Partial phonon densities of states (PDOS) of $CuGaX_2$ (X = S, Se, Te) as obtained from our VASP PBEsol calculations. The (red) dashed line represents the partial PDOS of Cu.

properties. The exchange-correlation energy was described with the generalized gradient approximation (GGA) with the PBEsol prescription.[28] A dense special ***k***-point sampling for the Brillouin zone (BZ) integration was performed in order to obtain well-converged energies and forces. More details of the *ab initio* electronic band structure calculations have been given, e.g., in Refs. 15 and 29. While most electronic calculations were performed without spin-orbit (SO) interaction, a few with the VASP code including SO interaction were also carried out in order to reveal possible effects of SO interaction on the lattice properties.[27,30] The effect of this interaction on the lattice parameters and dynamics was found to be insignificant and we therefore restrict the following discussion to results obtained without including SO coupling.

The $CuGaS_2$ and $AgGaS_2$ crystals investigated here were grown by a vapor phase transport technique using iodine as transport agent.[31] $AgGaSe_2$ and $AgGaTe_2$ samples have been grown from the elements using the horizontal freezing technique.[32,33]

The wavelength-modulated reflectivity spectra were obtained with a SPEX Model-1870 Czerny-Turner monochromator. A vibrating mirror near the entrance slit of the spectrometer generates wavelength-modulated radiation emerging from the exit slit. As a source for broadband optical spectroscopy, light emitting diodes (LEDs) possess many desired features which the incandescent and arc lamps lack.[34] In order to exploit these advantages a temperature-tuned LED source[35] was constructed to provide a bright, stable, and tunable radiation output with suitable LEDs.[36,37] The reflected radiation from the sample was detected with a UV-enhanced Si diode connected to a lock-in amplifier which also controls the vibrating mirror. The sample temperature was set with a continuous flow liquid helium cryostat equipped with fused quartz windows, from 5 K to 280 K in steps of 5 K. In order to obtain a stable temperature a heater installed inside the cryostat was used with a closed loop temperature controller. The temperature stability of this setup is ±0.5 K.

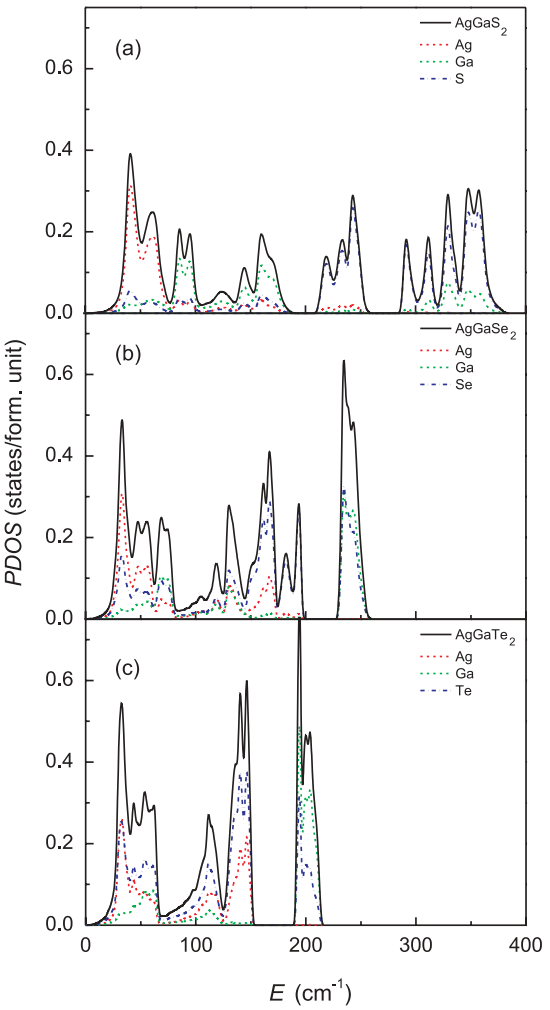

FIG. 7. (Color online) Partial phonon densities of states (PDOS) of $AgGaX_2$ (X = S, Se, Te) as obtained from our VASP PBEsol calculations. The (red) dashed line represents the partial PDOS of Ag.

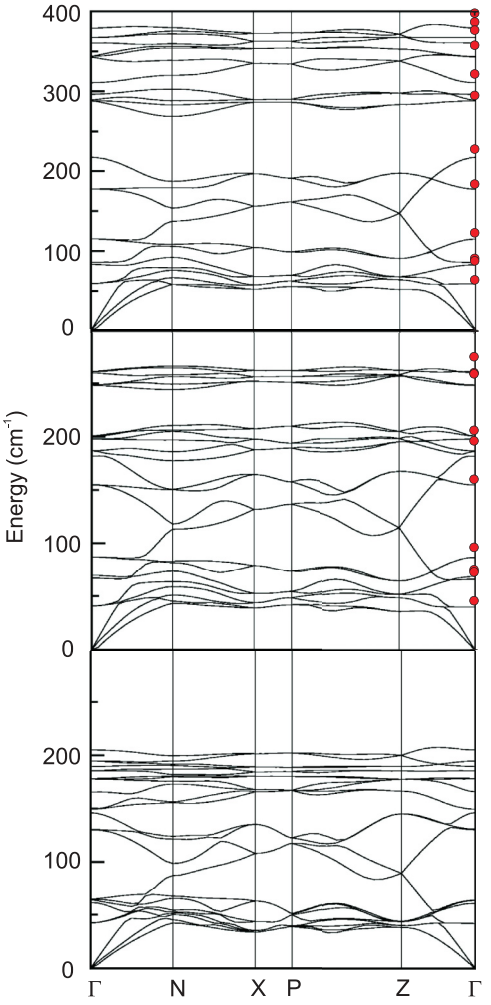

FIG. 8. (Color online) Phonon dispersion relations $CdGeP_2$, $CdGeAs_2$, and $ZnSnSb_2$, from top to bottom, respectively. The red circles are Γ-point Raman frequencies which have been taken from the literature. $CdGeP_2$: Data given in Table 3 (77 K) in Ref. 49; $CdGeAs_2$ taken from Table 2 in Ref. 48.

III. RESULTS AND DISCUSSION

The phonon dispersion relations and the PDOS of $CuGaS_2$ based on *ab initio* DFT-GGA calculations have been discussed before by us and other authors (cf. Ref. 15 and references therein). It appears that complete data for $CuGaSe_2$ and $CuGaTe_2$ are not available in the literature. Using *ab initio* codes Parlak *et al.* have calculated the phonon frequencies of $CuGaSe_2$ at the center of the Brillouin zone.[38] Semiempirical calculations based on the adiabatic bond charge model have also been published.[39] We display in Fig. 5 the phonon dispersion relations of $CuGaX_2$ (X = S, Se, Te) calculated by using the PBEsol approximation.[28] In Fig. 6 we show the related PDOS. When going from S via Se to Te, i.e., increasing the mass of the chalcogen, the overall energy scale is compressed and a gap seen for $CuGaS_2$ between 200 cm^{-1} and 260 cm^{-1} is gradually closed. For $CuGaS_2$ the acoustic phonons are dominated by Cu vibrations, whereas in $CuGaSe_2$ Cu and Se vibrations are equally important. For $CuGaTe_2$, however, the low-energy acoustic band is essentially Te like.

Ab initio calculations of the lattice properties of the $AgGaX_2$ (X = S, Se, Te) chalcopyrites have already been performed by several authors before using LDA codes for the exchange and correlation potential.[43,44] Our PBEsol calculations generally agree with the results of the preceding works. By comparing the calculated heat capacities of the $AgGaX_2$ compounds with our new experimental data we found that the low-temperature thermal properties are somewhat better described by using the PBEsol ansatz for the exchange and correlation potential. Details of the phonon dispersion relations of the $AgGaX_2$ compounds will be discussed with new low-temperature heat capacity data in a forthcoming paper.[45] Figure 7 shows the PDOS of the $AgGaX_2$ chalcopyrites calculated by using the PBEsol ansatz which have also been utilized in a recent work to calculate the low-temperature specific heats of several chalcopyrites.[46]

In order to explore the differences of the ternary chalcopyrites containing d-electron atoms (Cu and Ag) with those based on p-electron metal atoms like Cd or Zn, we

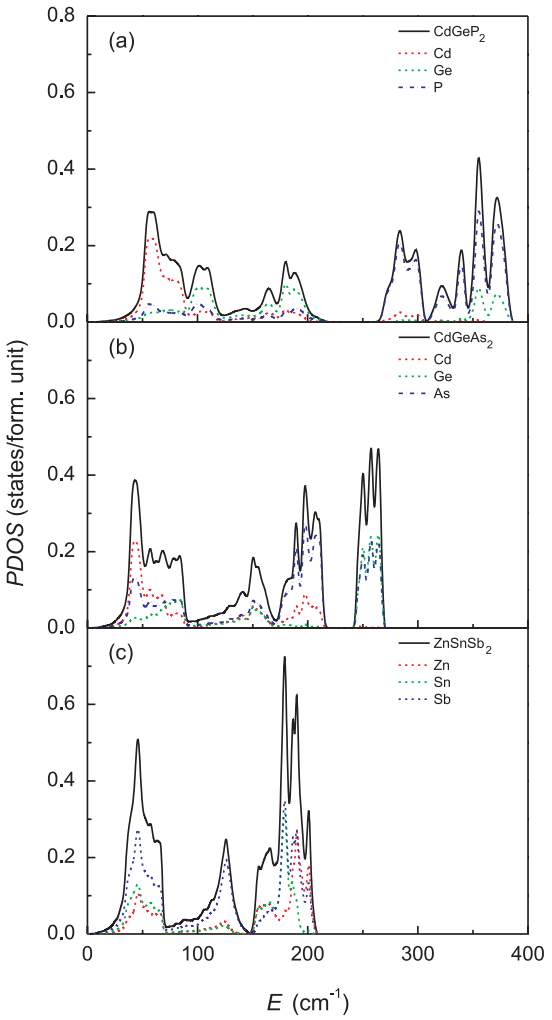

FIG. 9. (Color online) PDOS of MYX_2 (M = Zn, Cd; Y = Ge, Sn; X = P, As, Sb) as obtained from our VASP PBEsol calculations. The (red) dashed line represents the partial PDOS of Cd and Zn.

calculated the lattice dynamical properties and the PDOS of $CdGeP_2$, $CdGeAs_2$, and $ZnSnSb_2$ with the PBEsol approach. Semiempirical calculations of the phonon dispersion relations of $CdGeX_2$ (X = P, As) have been published before.[47,48] The lattice dynamical properties of $ZnSnSb_2$ have not been investigated yet. The results of our calculations are summarized in Figs. 8 and 9. The energy widths of the phonon dispersion bands are similar, when one replaces Cu by Zn or Ag by Cd. The acoustic phonons are either dominated by Cd-like vibrations ($CdGeP_2$ and $CdGeAs_2$) or by Sb-like vibrations for $ZnSnSb_2$.

Reflectance spectra were measured on samples of $CuGaS_2$ and on the series $AgGaX_2$ (X = S, Se, Te) as a function of the temperature. $CuGaS_2$ exhibits three edge excitons, two (B and C) near ~2.64 eV (at $T = 0$ K) and one (A) at 2.50 eV. Their intensities, linewidths, and energies are temperature dependent; the latter decreases with increasing temperature (see details for the B and C excitons in Fig. 10). At low temperatures two well-resolved peaks of about equal width and slightly different intensity, separated by about 10 meV, are

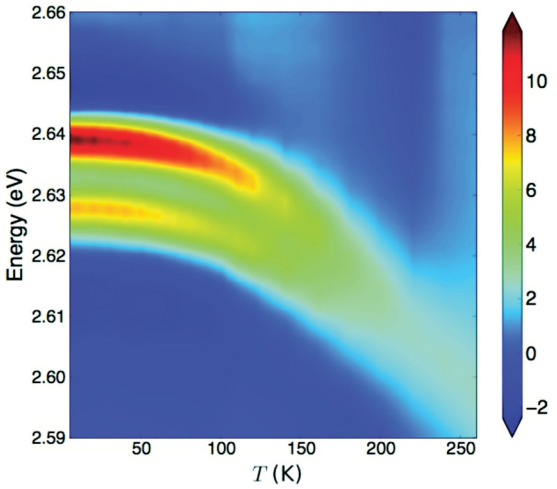

FIG. 10. (Color online) Evolution with temperature of the wavelength-modulated reflectivity spectra of $CuGaS_2$ showing the B, C excitons near 2.64 eV.

seen near 2.64 eV. With increasing temperature due to the rapid increase of their linewidths they overlap above ~100 K and form one broad band at room temperature. Figure 10 shows the temperature dependence of the energy of the two exciton peaks near 2.64 eV versus temperature. Our dependence of the exciton A [see Fig. 11(a)] is in good agreement with data obtained before by Choi and Yu and more recently by Levcenco *et al.*[12,50]

Whereas in the cubic monohalides of copper, CuX (X = Cl, Br, I), the edge exciton is split into a quadruplet ($J = 3/2$) and a doublet ($J = 1/2$), in the tetragonal chalcopyrites the $J = 3/2$ quadruplet splits into two doublets and consequently three exciton doublets are observed. The splitting results from a combination of spin-orbit and crystal field interaction. The B-C doublet splitting shown in Fig. 11 amounts to ~10 meV which corresponds predominantly to spin-orbit splitting.[51,52] The A (B, C) splitting (~120 meV) corresponds predominantly to the crystal field.

Energy, intensity, and linewidth (half-width at half maximum), e.g., of the B and C excitons, have been determined by fitting the second derivative of two Lorentzian resonance lines. A characteristic fit is shown in the inset in Fig. 11(a). Figure 11 compiles our new data obtained for $CuGaS_2$ and compares them with literature data for $CuGaSe_2$ and $CuGaTe_2$.[53,54]

The temperature dependence of the exciton energies of all $CuGaX_2$ chalcopyrites shown in Fig. 11 was initially analyzed by fitting a single Bose-Einstein frequency according to

$$E(T) = E_0 + A_1[2n_{\mathrm{BE}}(E_1/k_{\mathrm{B}}T) + 1], \qquad (1)$$

where A_1 is the weight which, if negative, describes the degree of the energy decrease with increasing temperature and n_B is the Bose-Einstein factor:

$$n_{\mathrm{BE}}(E_1/k_{\mathrm{B}}T) = 1/[\exp(E_1/k_{\mathrm{B}}T) - 1]. \qquad (2)$$

The fitted energies E_0, E_1 and the weight A_1 are summarized in Table II.

A comparison of the temperature dependence of the gap energies of $CuGaS_2$, $CuGaSe_2$, and $CuGaTe_2$ reveals

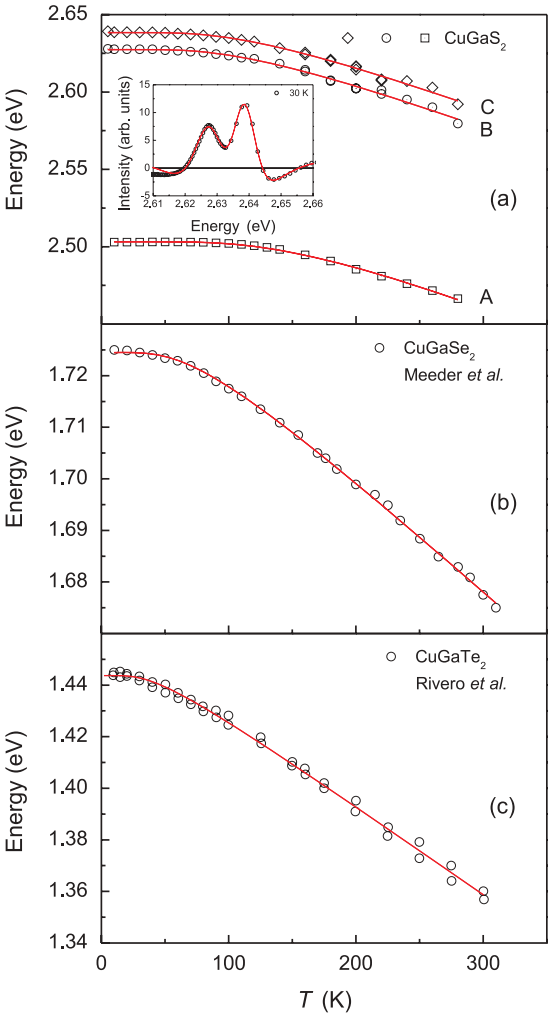

FIG. 11. (Color online) Exciton energies of (a) $CuGaS_2$ (our data), (b) $CuGaSe_2$ (Ref. 53), and (c) $CuGaTe_2$ (Ref. 54). The (red) solid lines represent fits with Eq. (1). The fitted parameters are summarized in Table II. The inset in (a) shows the 30 K spectrum (excitons B and C of $CuGaS_2$) with a fit (red) solid line of the second derivative of a Lorentzian resonance line.

a remarkable trend. $CuGaS_2$ shows a broad plateau below ∼100 K. This plateau is less pronounced for $CuGaSe_2$ and the temperature dependence of the gap energy of $CuGaTe_2$

TABLE II. Compilation of the parameters obtained from a fit of a single Bose-Einstein frequency, according to Eq. (1), to the experimental data of $CuGaX_2$ (X = S, Se, Te) displayed in Fig. 11. The $CuGaS_2$ data have been measured in this work; the data of $CuGaSe_2$ and $CuGaTe_2$ have been taken from Meeder *et al.* and Rivero *et al.*, respectively (Refs. 53,54).

	E_0 (eV)	A_1 (eV)	E_1 (K)
$CuGaS_2$ (A)	2.592(6)	−0.088(6)	488(14)
$CuGaS_2$ (B)	2.682(7)	−0.054(7)	343(24)
$CuGaS_2$ (C)	2.694(7)	−0.056(7)	353(25)
$CuGaSe_2$	1.748(1)	−0.023(1)	208(7)
$CuGaTe_2$	1.464(2)	−0.020(2)	116(10)

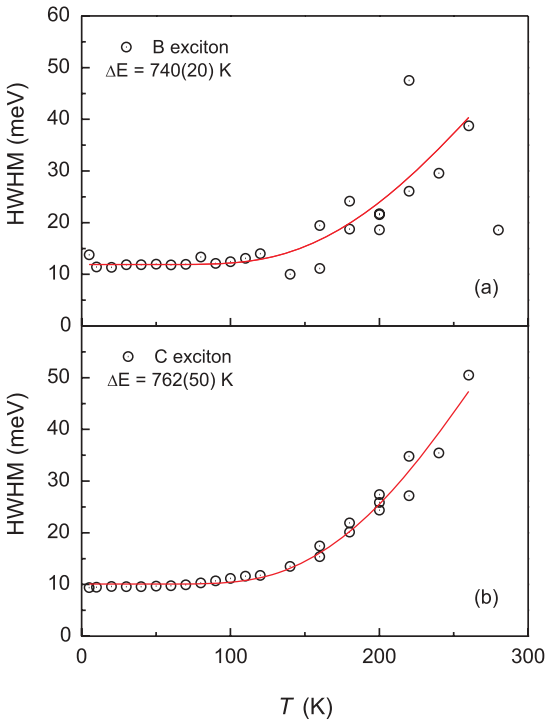

FIG. 12. (Color online) Linewidth (HWHM) of the excitons B and C of $CuGaS_2$ resulting from fits of the second derivative of two superposed Lorentzian resonance lines to the spectra.

resembles a linear decrease with almost no plateau left at low temperatures. Accordingly, the energies of the Bose-Einstein oscillators steadily decrease as sulfur is replaced by selenium and tellurium. We will demonstrate below that the extended plateau in the low-temperature regime observed for $CuGaS_2$ can be modeled by an additional low-frequency Bose-Einstein oscillator with a positive weight, i.e., an increase of the gap energy with increasing frequency.

Before we compare the results obtained for $CuGaX_2$ with those of our new measurements on $AgGaS_2$ and $AgGaSe_2$ we briefly discuss the linewidth of the excitons B and C of $CuGaS_2$ shown in Fig. 12. The temperature dependence of the linewidths can be well described by including a residual linewidth W_0, due to defects and acoustic phonons, a linear increase due to relaxation via acoustic phonons and/or defects, and an exponential term due to relaxation via optical phonons,[55,56]

$$\Delta W(T) = \Delta W_0 + \alpha\, T + \beta\, \exp(\Omega/k_{\mathrm{B}}T), \qquad (3)$$

where $\Delta W(T)$ is the linewidth (HWHM), W_0 is the residual linewidth, and α and β describe the linear and exponential increase of the exciton linewidth, the latter with an activation energy Ω.

On average the excitation energies Ω amount to ∼750 K and the linear increase at low temperatures was found unnecessary. The centers of the optical phonon bands lie at ∼500 K[15] somewhat below the corresponding excitation energies. At the moment we are not able to fathom the origin of this difference.

In view of the nonmonotonic temperature dependence of gap energies for the $AgGaX_2$ (X = S, Se, Te) observed by several authors previously, we decided to redetermine, with

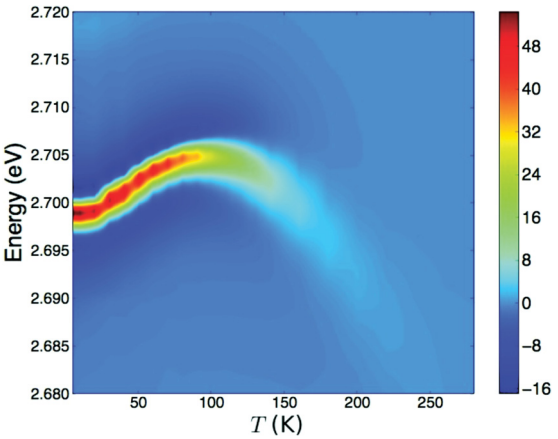

FIG. 13. (Color online) Evolution with temperature of the wavelength-modulated reflectivity spectra of $AgGaS_2$.

improved resolution, the temperature dependence of the gaps of $AgGaS_2$ and $AgGaSe_2$ using the wavelength-modulated reflectivity setup described above. A particularly impressive representation of the temperature dependence of the energy and the intensity of the edge exciton of $AgGaS_2$ is shown in Fig. 13.

Figure 14 displays the gap energies of $AgGaS_2$ and $CuGaS_2$ versus T. The nonmonotonic behavior of the gap of $AgGaS_2$ found previously[13] is confirmed; however its description in

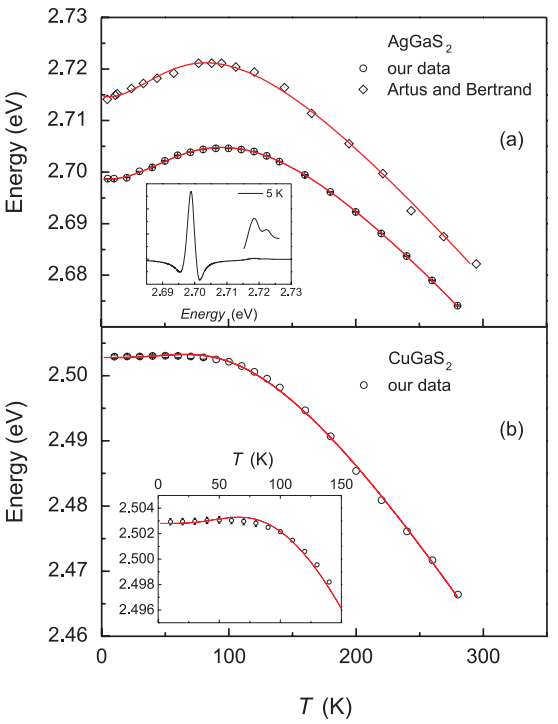

FIG. 14. (Color online) Temperature dependence of the gap energy of (a) $AgGaS_2$ (our data and those of Artus and Bertrand[13]) and (b) $CuGaS_2$. The (red) solid lines represent the fits to Eq. (4) assuming two Bose-Einstein oscillators. The inset in (a) displays the wavelength-modulated reflectivity spectrum at 5 K. The strength of the B and C excitons has been enlarged by a factor of 20 and upshifted for clarity. The inset in (b) highlights the low-temperature part of the gap temperature dependence.

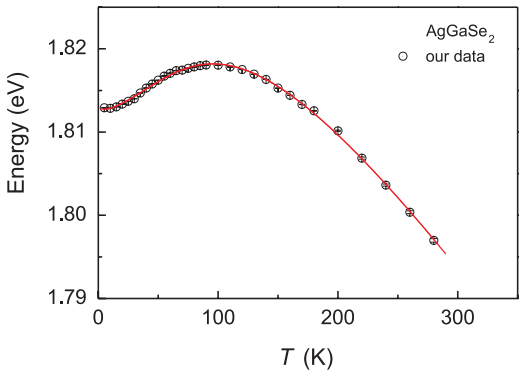

FIG. 15. (Color online) Temperature dependence of the gap energy of (o) $AgGaSe_2$ fitted with Eq. (4) which assumes two Bose-Einstein oscillators [(red) solid line].

terms of a linear behavior below and above the maximum has to be modified. Approaching $T \to 0$ K we clearly observe a leveling-off to a constant value and above the maximum the temperature dependence is not linear. In order to describe the temperature dependence we extended Eq. (1) by adding the contributions of low-energy phonons with opposite weight leading to an increase of the gap energy according to[5,6]

$$E(T) = E_0 + \sum_i A_i [2n_{\mathrm{BE}}(E_i/k_{\mathrm{B}}T) + 1], \qquad (4)$$

where the parameters have the same meaning as in Eq. (1). In Fig. 14 we show for comparison also an analysis of the gap energy of $CuGaS_2$ with two Bose-Einstein oscillators following Eq. (4). Data and fits for $AgGaSe_2$ are shown in Fig. 15. The fit parameters are summarized in Table III.

As has already been discussed in the literature, preparation of samples of $AgGaTe_2$ giving good quality optical spectra proves to be difficult and, consequently, a wide variation of the band gaps ranging from 0.99 eV to 1.32 eV has been reported.[23,24,57–59]

With the available samples we were able to collect data only up to 100 K. In Fig. 4(b) we display some of these data in comparison with those extant in the literature. Our data, together with those in the literature, display a shallow maximum between 50 K and 80 K, which can be described by the two-oscillator model with frequencies consistent with the phonon dispersion relations.

As we have shown before, the temperature dependence of the gaps of the chalcopyrites MYX_2 (M = Zn, Cd; Y = Ge, Sn) which do not involve p-d electron hybridization can be fitted with a *single* Bose-Einstein oscillator with energies compiled

TABLE III. Compilation of the parameters obtained by fitting our experimental data in Figs. 14 and 15 with two Bose-Einstein oscillators E_i ($i = 1, 2$) according to Eq. (4).

		E_0 (eV)	A_1 (eV)	E_1 (K)	A_2 (eV)	E_2 (K)
$AgGaS_2$	Artus[a]	2.784(6)	−0.074(5)	313(35)	0.004(4)	47(31)
$AgGaS_2$	our data	2.783(2)	−0.088(1)	395(2)	0.0036(5)	56(2)
$CuGaS_2$	our data	2.579(4)	−0.078(3)	425(17)	0.002(5)	120
$AgGaSe_2$	our data	1.871(2)	−0.060(2)	379(10)	0.0018(5)	36(8)

[a]Reference 13.

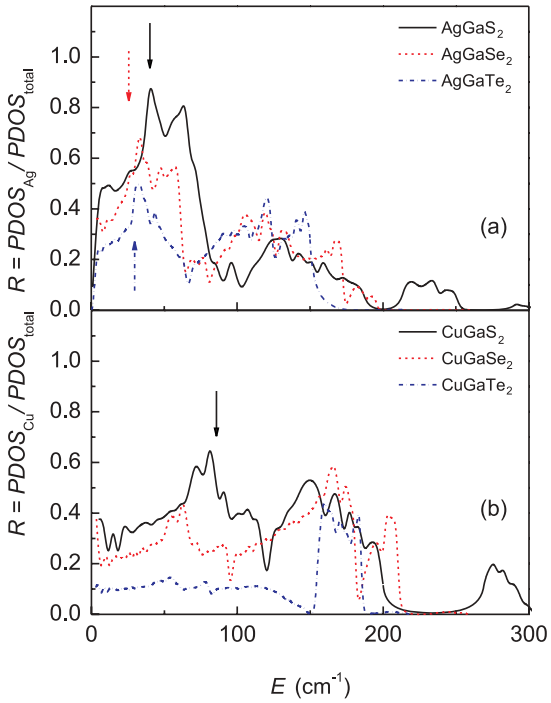

FIG. 16. (Color online) Ratio of the partial PDOS of (a) Ag and (b) Cu with respecct to the total PDOS of $MGaS_2$, $MGaSe_2$, and $MGaTe_2$ (M = Cu, Ag), with (black) solid, (red) dashed, and (blue) dash-dotted lines, respectively. The vertical arrows indicate the energies of the second low-energy Bose-Einstein oscillator (E_2) obtained by fitting the temperature dependence of the energy gaps with Eq. (4) (see Table III).

in Table I. The nonmonotonic temperature dependence of the gap of $AgGaX_2$ requires two Bose-Einstein oscillators with coupling constants of opposite sign. The frequencies of the Bose-Einstein oscillators correspond to optic and acoustic phonons, the latter essentially Ag like. The broad plateau of the gap energy dependence of $CuGaS_2$ can also be ascribed to a second low-energy Bose-Einstein oscillator of an energy agreeing well with the Cu maximum in the partial PDOS. The need for two oscillators is not immediately obvious for $CuGaSe_2$ and $CuGaTe_2$ (see Fig. 11). Figure 16 displays the ratios of the Ag and Cu partial PDOS divided by the total PDOS. Additionally, we have marked by vertical arrows the respective energies of the low-energy Bose-Einstein oscillator which accounts for the gap increase at low temperatures.

IV. SUMMARY AND CONCLUSIONS

As already surmised previously,[1] the temperature dependence of the energy gaps of semiconductors is due to electron-phonon interaction. In this paper we investigated such dependence for a series of tetrahedral semiconductors of the chalcopyrite family. Since the phonon dispersion relations and densities of states of many of these materials were not known, we have calculated by *ab initio* techniques several of these phonons so as to relate them to the measured temperature dependence of the gaps. Although calculations of the temperature dependence of the gaps based on semiempirical electron-phonon interaction have appeared in the literature,[60] thus far no calculations for ternary materials have been performed. In this paper we present fits to the measured temperature dependence of the electronic gaps based on representations of the corresponding phonons by means of Bose-Einstein oscillators: Two such oscillators usually suffice to produce excellent agreement. Remarkably, in some cases the gap energies increase with temperature while in others they decrease. Such nonmonotonic behavior is particularly apparent in materials involving Cu and Ag as cations. Unfortunately, no *ab initio* calculations describing this behavior are available as yet. We hope that the systematic analysis presented here will encourage theorists to tackle the peculiar problem of temperature dependence of the electronic gaps of semiconductors involving d-electron atoms (e.g., Cu or Ag) in the valence band. Measurements at low temperatures using crystals with pairwise replacement of isotopes (e.g., $AgGa^{32}S_2$-$AgGa^{34}S_2$; $Ag^{69}GaS_2$-$Ag^{71}GaS_2$; $^{107}AgGaS_2$-$^{109}AgGaS_2$) would help to separate the individual effects of the various atoms on the zero-temperature gap renormalization.

ACKNOWLEDGMENTS

A.H.R. has been supported by CONACYT Mexico under Project No. 152153 PPPROALMEX-DAAD-CONACYT and by a Marie-Curie Intra-European Fellowship. A.M. acknowledges financial support from the Spanish MCYT under Grants No. MAT2010-21270-C04-03 and No. CSD2007-00045 and the supercomputer resources provided by the Red Española de Supercomputación. We are grateful to Y. Pouillon and O. Castillo for valuable technical and computational support. Work carried out at Purdue has been supported by the US National Science Foundation under Grant No. DMR 0705793. J.S.B. and A.K.R. thank H. Alawadhi, University of Sharjah, United Arab Emirates, for discussions and I. Miotkowski for growing some of the bulk $AgGaS_2$ samples.

*Corresponding author: rekre@fkf.mpg.de

[1] M. Cardona and M. L. W. Thewalt, Rev. Mod. Phys. **77**, 1173 (2005).
[2] S. Zollner, S. Gopalan, and M. Cardona, Solid State Commun. **77**, 485 (1991).
[3] D. Olguín, A. Cantarero, and M. Cardona, Phys. Status Solidi B **220**, 33 (2000).
[4] A. Marini, Phys. Rev. Lett. **101**, 106405 (2008).
[5] A. Göbel, T. Ruf, M. Cardona, C. T. Lin, J. Wrzesinski, M. Steube, K. Reimann, J.-C. Merle, and M. Joucla, Phys. Rev. B **57**, 15183 (1998).
[6] J. Serrano, Ch. Schweitzer, C. T. Lin, K. Reimann, M. Cardona, and D. Fröhlich, Phys. Rev. B **65**, 125110 (2002).
[7] A. Manoogian and A. Leclerc, Phys. Status Solidi B **92**, 23 (1979).
[8] Y. P. Varshni, Physica **34**, 149 (1967).
[9] A. Manoogian and J. C. Woolley, Can. J. Phys. **62**, 285 (1984).

[10]R. Pässler, Phys. Status Solidi B **200**, 155 (1997).
[11]L. I. Berger, L. V. Kradinova, V. M. Petrov, and V. D. Prochukhan, Inorg. Mater. **9**, 1258 (1973).
[12]S. Levcenco, S. Doka, V. Tezlevan, D. Fuertes Marron, L. Kulyuk, T. Schedel-Niedrig, M. Ch. Lux-Steiner, and E. Arushanov, Physica B **405**, 3547 (2010).
[13]L. Artus and Y. Bertrand, Solid State Commun. **61**, 733 (1987).
[14]F. Herman and S. Skillman, *Atomic Structure Calculations* (Prentice-Hall, Inc., Inglewood Cliffs, New Jersey, 1963).
[15]A. H. Romero, M. Cardona, R. K. Kremer, R. Lauck, G. Siegle, C. Hoch, A. Muñoz, and A. Schindler, Phys. Rev. B **83**, 195208 (2011).
[16]I. H. Choi, D. H. Lee, Y. D. Choi, Y. M. Yu, and P. Y. Yu, J. Korean Phys. Soc. **44**, 403 (2004).
[17]R. Madelon, M. Shaimi, A. Hairie, E. Paumier, and B. Mercey, Solid State Commun. **50**, 545 (1984).
[18]S. Ozaki, M. Sasaki, and S. Adachi, Phys. Status Solidi A **203**, 2648 (2006).
[19]E. Calderón, B. Fernández, L. Durán, P. Grima, M. Morocoima, E. Quintero, C. Rincón, and M. Quintero, Physica **404**, 4095 (2009).
[20]W. Scott, J. Appl. Phys. **44**, 5165 (1973).
[21]L. I. Berger, L. V. Kradinova, V. M. Petrov, and V. D. Prochukhan, Izv. Akad. Nauk. SSSR Neorg. Mater. **9**, 1258 (1973) [Inorg. Mater. (USSR) **9**, 1118 (1973)].
[22]T. Raadik, J. Krustok, and M. V. Yakushev, Physica B **406**, 418 (2011).
[23]I. V. Bodnar, V. F. Gremenok, R. W. Martin, and M. V. Yakushev, Opt. Spectra **88**, 377 (2000).
[24]J. Krustok, A. Jagomägi, M. Grossberg, J. Raudoja, and M. Danilson, Solar Energy Materials and Solar Cells **90**, 1973 (2006).
[25]G. Kresse and J. Furthmüller, Comput. Mater. Sci. **6**, 15 (1996).
[26]P. E. Blöchl, Phys. Rev. B **50**, 17953 (1994).
[27]G. Kresse and D. K. Joubert, Phys. Rev. B **59**, 1758 (1999), and references therein.
[28]J. P. Perdew, A. Ruzsinszky, G. I. Csonka, O. A. Vydrov, G. E. Scuseria, L. A. Constantin, X. L. Zhou, and K. Burke, Phys. Rev. Lett. **100**, 136406 (2008).
[29]M. Cardona, R. K. Kremer, G. Siegle, A. Muñoz, A. H. Romero, and M. Schmidt, Phys. Rev. B **82**, 085210 (2010).
[30]L. E. Díaz-Sánchez, A. H. Romero, M. Cardona, R. K. Kremer, and X. Gonze, Phys. Rev. Lett. **99**, 165504 (2007).
[31]R. Lauck, J. Cryst. Growth **312**, 3642 (2010).
[32]P. G. Schunemann, S. D. Setzler, T. M. Pollak, M. C. Ohmer, J. T. Goldstein, and D. E. Zelmon, J. Cryst. Growth **211**, 242 (2000).
[33]A. Burger, J.-O. Ndap, Y. Cui, U. Roy, S. Morgan, K. Chattopadhyay, X. Ma, K. Faris, S. Thibaud, R. Miles, H. Mateen, J. T. Goldstein, and C. J. Rawn, J. Cryst. Growth **225**, 505 (2001).
[34]With the current state of the art LEDs offer significant improvement over conventional sources for wavelength-modulated spectroscopy due to their high brightness and efficiency along with their small size and low cost. Bright LEDs are commercially available covering the spectral region from 1000 nm to 365 nm with successive spectral intensity peaks of the LEDs as close as 20 nm.
[35]J. S. Bhosale, Rev. Sci. Instrum. **82**, 093103 (2011).
[36]Golden DRAGON LED, OSRAM Opto Semiconductors, Inc., 2650 San Tomas Expressway, Suite 200, Santa Clara, CA 95051 (2011).
[37]LZ1 High Efficacy LED Emitter, LED Engin, Inc., 3350 Scott Blvd., Bldg. 9, Santa Clara, CA 95054 (2012).
[38]C. Parlak and R. Eryiğit, Phys. Rev. B **73**, 245217 (2006).
[39]T. Gürel and R. Eryiğit, Cryst. Res. Technol. **41**, 83 (2006).
[40]M. Akdoğan and R. Eryiğit, J. Phys.: Condens. Matter **14**, 7493 (2002).
[41]F. W. Ohrendorf and H. Haeuseler, Cryst. Res. Technol. **34**, 339 (1999).
[42]V. Riede, H. Sobotta, H. Neumann, and H. X. Nguyen, Solid State Commun. **28**, 449 (1978).
[43]J. Łażewski and K. Parlinski, J. Phys.: Condens. Matter **11**, 9673 (1999).
[44]J. Łażewski and K. Parlinski, J. Chem. Phys. **114**, 6734 (2001).
[45]R. K. Kremer *et al.* (unpublished).
[46]M. Cardona, R. K. Kremer, R. Lauck, A. H. Romero, A. Muñoz, and A. Burger, in Phonons 2012: 14th Int. Conf. on Phonon Scattering in Condensed Matter (to be published).
[47]Semiempirical force field calculations of the phonon dispersion relations of $CdGeP_2$ have been published by J. Łażewski and K. Parlinski, Phys. Status Solidi B **218**, 411 (2000). Their data are in agreement with our findings.
[48]J. Pujol, L. Artus, J. Pascual, and J. Camassel, Physica Scripta **41**, 696 (1990).
[49]L. Artus, J. Pascual, J. Pujol, J. Camassel, and R. S. Feigelson, Phys. Rev. B **43**, 2088 (1991).
[50]I.-H. Choi and P. Y. Yu, J. Phys. Chem. Solids **57**, 1695 (1996).
[51]A. S. Poplavnoi and Yu. I. Polygalov, Inorg. Mater. **7**, 1527 (1971).
[52]N. N. Syrbu, I. M. Tiginyanu, L. L. Nemerenco, V. V. Ursaki, V. E. Tezlevan, and V. V. Zalamai, J. Phys. Chem. Solids **66**, 1974 (2005).
[53]A. Meeder, A. Jäger-Waldau, V. Tezlevan, E. Arushanov, T. Schedel-Niedrig, and M. Ch. Lux-Steiner, J. Phys.: Condens. Matter **15**, 6219 (2003).
[54]A. Rivero, M. Quintero, Ch. Power, J. Gonzalez, R. Tovar, and J. Ruiz, J. Electron. Mater. **26**, 1428 (1997).
[55]P. Y. Yu and M. Cardona, *Fundamentals of Semiconductors*, 4th ed. (Springer, Heidelberg, 2010).
[56]M. N. Nordin, Juerong Li, S. K. Clowes, and R. J. Curry, Nanotechnology **23**, 275701 (2012).
[57]U. N. Roy, B. Mekonen, O. O. Adetunji, K. Chattopahhyay, F. Kochari, Y. Cui, A. Burger, and J. T. Goldstein, J. Cryst. Growth **241**, 135 (2002).
[58]R. Kumar and R. K. Bedi, J. Mater. Sci. **40**, 455 (2005).
[59]S. Arai, S. Ozaki, and S. Adachi, Appl. Opt. **49**, 829 (2010). A fit of the temperature dependence of the gaps measured by optical absorption (cf. Fig. 1 in this work) with a single Bose-Einstein oscillator results in a frequency of $\sim$220 cm^{-1} in good agreement with the energy of the optical phonons (cf. Fig. 7). A maximum and a decrease of the band gap towards lowest temperatures, however, has not been found by Arai *et al.*
[60]D. Olguín, M. Cardona, and A. Cantarero, Solid State Commun. **122**, 575 (2002).